*Journal of the European Ceramic Society* **16** (1996) 1083–1088

PII: S0955-2219(96)00033-7
0955-2219/96/$15.00

# Development of High-Strength Whiteware Bodies

Soumen Maity[a] & B. K. Sarkar[b]

[a]Central Glass & Ceramic Research Institute, P.O. Jadavpur, Calcutta–700 032, India
[b]Indian Association for Cultivation of Science, P.O. Jadavpur, Calcutta–700 032, India

(Received 15 November 1995; revised version received 16 January 1996; accepted 23 January 1996)

***Abstract***

*The effect of sillimanite sand as a replacement for quartz and alumina/cordierite glass-ceramic for feldspar was studied. Compositional variations were due to the gradual incorporation of alumina in place of cordierite glass-ceramic. Increased replacement of cordierite glass-ceramic by alumina (20%) increased the flexural strength by 100%, giving a value of 195 MPa. Elastic modulus, microhardness and fracture toughness also showed sharp increases compared with values for conventional triaxial whiteware compositions. Improvement in mechanical properties was attributed to the presence of sillimanite and alumina particles present as fracture-resistant dispersoids in a viscous glassy matrix. Increased fracture behaviour is due to minimization of the glassy phase and limiting the size of Griffith's flaws. © 1996 Elsevier Science Limited.*

## 1 Introduction

In recent years the electrical porcelain industry has been looking for higher mechanical strengths. The oldest bodies and those in most common use today are the felspathic porcelains made from clay, quartz and feldspar. Feldspar acts as a flux and quartz imparts rigidity to the wares. However, the unreacted residual quartz adversely affects the thermomechanical properties due to development of internal stresses in the glassy phase during phase transformation.

The function of quartz in the strength of a whiteware body is a subject of dispute. Some authors assume that quartz particles introduce a prestress in the overall body whereby the glass matrix is put into compression, thereby increasing strength.[1–4] Others oppose this theory.[5–7] Experimental evidence on both views is abundant but remains inconclusive.

Mullite content and its morphology have also been shown to affect the mechanical properties. It was reported[8,9] that the strength increased with increasing mullite content but that firing at high temperature coarsened the mullite and, as a consequence, the strength decreased.

Considerable improvement in the strength was also achieved by reducing the particle size of the quartz to the range 10–30 $\mu$m.[1,7] Attempts were also made to substitute quartz by non-conventional materials like alumina,[10,11] zircon,[12] alumino-silicates[13–15] and crystallizing glass,[16] resulting in fruitful compositions. It was also shown[17] that a dispersion-strengthened glass matrix with high-strength particles dispersed within the glass will limit the size of the Griffith flaw, thereby increasing the strength.

Fluxing of porcelain bodies with feldspar results in glass with brittle fracture character. In this study feldspar was substituted by cordierite-based crystallizing glass possessing low thermal expansion and high thermal shock resistance. Also, quartz was fully substituted by sillimanite sand in an attempt to reduce the microstress. The advantage of using sillimanite is twofold. Firstly, it is a waste material and is abundantly available. Secondly, being a volume-stable and highly fracture-resistant phase, it would result in improved mechanical properties. Alumina was substituted in place of cordierite glass-ceramic to further improve the mechanical properties.

## 2 Experimental Procedure

### 2.1 Raw materials

Raw materials used in the present investigation were china clay (Rajmahal, Bihar), talc (Jaipur, Rajasthan), feldspar (Rajmahal, Bihar), quartz (Ranchi, Bihar), calcined alumina (INDAL Co. Ltd), beach sand sillimanite (a by-product obtained after separation of zircon, rare earths and other minerals from beach sand in Kerala) and reagent-grade $TiO_2$. All the above materials were procured in ground form of at least –250 mesh (75 $\mu$m) size. X-ray powder diffraction (XRD) phase analysis and chemical analysis of the raw materials, given in Tables 1 and 2 respectively, confirmed that the impurities present were within the compositional range, and thus would not grossly affect the fired properties.

**Table 1.** XRD analysis of raw materials

| *Raw materials* | *Major phase* | *Minor phase* |
|---|---|---|
| China clay | Kaolinite | Muscovite, rutile, quartz, illite |
| Quartz | Quartz | Rutile |
| Feldspar | Orthoclase | Illite, muscovite |
| Talc | Talc | Quartz, illite |
| Alumina | Corundum | |
| Sillimanite sand | Sillimanite | Quartz, zircon |
| Titanium dioxide | Anatase | |

**Table 2.** Chemical analysis of raw materials

| *Constituents (wt%)* | *China Clay* | *Feldspar* | *Talc* | *Quartz* | *Calcined alumina* | *Sillimanite sand* | *Titania* |
|---|---|---|---|---|---|---|---|
| $SiO_2$ | 47·63 | 65·63 | 63·29 | 99·06 | 0·09 | 37·50 | 0·38 |
| $Al_2O_3$ | 37·89 | 19·19 | 0·76 | 0·30 | 99·93 | 59·78 | Tr |
| $Fe_2O_3$ | 0·56 | 0·17 | 0·39 | 0·19 | 0·06 | 0·37 | 0·27 |
| CaO | 0·48 | Tr | Tr | 0·23 | Tr | 0·52 | 0·32 |
| MgO | 0·13 | 0·49 | 31·56 | Tr | Tr | 0·50 | 0·34 |
| $Na_2O$ | 0·10 | 3·56 | 0·82 | 0·06 | 0·05 | 0·07 | 0·10 |
| $K_2O$ | 0·18 | 10·42 | 0·06 | 0·09 | – | 0·04 | 0·26 |
| $TiO_2$ | 0·61 | Tr | Tr | Tr | Tr | 0·76 | 98·01 |
| L.O.I | 12·42 | 0·65 | 1·80 | 0·28 | – | 0·30 | 0·32 |

The glass-ceramic used in the present investigation was essentially of cordierite composition. Raw materials used were 37% china clay, 32% talc, 12% feldspar, 9% calcined alumina and 10% $TiO_2$ as a nucleating agent. Raw mixes were melted in an electric furnace and cooled for nucleation and growth of crystalline constituents. XRD analysis confirmed the presence of $\alpha$-cordierite as the principal constituent. The nucleated powder was ground and added as a replacement for feldspar.

### 2.2 Sample preparation

Respective batch compositions (Table 3) were mixed in the required proportions and wet-milled in porcelain pots for 20 h with porcelain grinding media. Resultant slurries were passed over a magnetic separator to remove iron contamination and sieved through –300 mesh (50 $\mu$m). They were further dried in Plaster of Paris moulds, just enough to make them amenable to extrusion. This was done to retain the plasticity of the clay. Previous experience with oven-dried powders did not give good results during extrusion as oven drying at 110°C for 24 h destroyed the plastic nature of clay mixes. Mould-dried compositions were further aged in a moist atmosphere for regaining additional plasticity.

Mixes were extruded in a vacuum extruder twice for thorough mixing. Resultant kneaded mixes were extruded in the form of cylindrical rods 6·0 cm in length and 0·8 cm diameter. After air drying at room temperature for 24 h they were further dried in an oven for 24 h at a temperature of 110°C.

Samples were biscuit fired at 1000°C and were again ground and milled to powder of –300 mesh. Resultant powders were uniaxially pressed in the form of rectangular bars of dimensions 9·0 × 1·0 × 1·0 cm. They were oven dried and machined to cylindrical rods of 5·0 cm length with a diameter of 0·7 cm prior to firing.

### 2.3 Measurements

Density and porosity of fired samples were determined by Archimedes' immersion technique, involving boiling in water for 2 h and a further soaking of 24 h at ambient temperature. Relative densities of the fired test bars were determined from the bulk densities divided by their respective true densities. True densities were calculated by the law of averages.

Bending strength was measured using an electromechanical universal tester (Instron 1195) in a four-point bending fixture. The crosshead speed was 2 mm $min^{-1}$ with an inner and outer span of 20 and 40 mm, respectively.

**Table 3.** Raw material composition (wt%) used in the batches

| *Raw material* | *Batch* | | | | |
|---|---|---|---|---|---|
| | $S_{15}$ | $A_0$ | $A_{10}$ | $A_{15}$ | $A_{20}$ |
| China clay | 50 | 50 | 50 | 50 | 50 |
| Sillimanite sand | 25 | 25 | 25 | 25 | 25 |
| Cordierite glass-ceramic | 15 | 25 | 15 | 10 | 5 |
| Alumina | – | – | 10 | 15 | 20 |
| Quartz | 10 | – | – | – | – |

Modulus of elasticity was measured by the pulse–echo method by an ultrasonic tester (USIP 12).

Microhardness and fracture toughness were measured on mirror polished surface by the indentation technique in a Vickers microhardness tester (Shimadzu HMV 2000). For each case a mean of 10 measurements was taken. Fracture toughness was calculated from the formula given by Evans and Wilshaw.[18]

## 3 Results and Discussion

### 3.1 Vitrification behaviour

Five batch compositions (Table 3) of porcelain bodies were fired between 1250 and 1550°C and the fired linear shrinkage, apparent porosity and bulk density measured to determine the vitrification behaviour. Results are shown in Fig. 1. Upon firing, all the properties measured showed the trend typical of conventional porcelain compositions.

From Fig. 1 it is apparent that, in the present compositions, the porosity decreases with increasing firing temperature, with a corresponding rise in linear shrinkage and bulk density values. Optimum vitrification was achieved when the apparent porosity reached a minimum value tending to be nearly zero. Firing above the vitrified range resulted in a drastic fall of the physical properties due to forced expulsion of the entrapped gases, resulting in 'blisters' and 'bloating'. Samples with increased alumina content vitrified at higher temperatures, giving greater shrinkage values due to elimination of porosity. Increase in shrinkage values also ensured more complete wetting and densification of the individual grains during the vitrification process.

Differences in density of vitrified products is brought about primarily by the changes in porosity and the presence/formation of phases with varied densities. Correctly fired hard porcelain is non-porous in the sense that it is vacuum-tight and does not de-gas. On the other hand, it is porous as it has a number of closed unconnected pores, indicated by the difference between bulk and true powder densities. With increased replacement of cordierite glass-ceramic by alumina, bulk density increased with the rate decreasing comparatively at higher alumina (20%) content. Apparent porosity showed an inverse relation with bulk density, as expected.

Increase in bulk density resulted from the progressive addition of higher density alumina (3·98 g $cm^{-3}$) in place of nucleated cordierite (2·65 g $cm^{-3}$) and also due to less formation of closed pores. Addition of 15% quartz in place of alumina, however, increased the apparent porosity in vitrified samples. This was due to non-wettability of the crystalline phases by the lower amount of liquid phase formed. Simultaneously the bulk density also decreased.

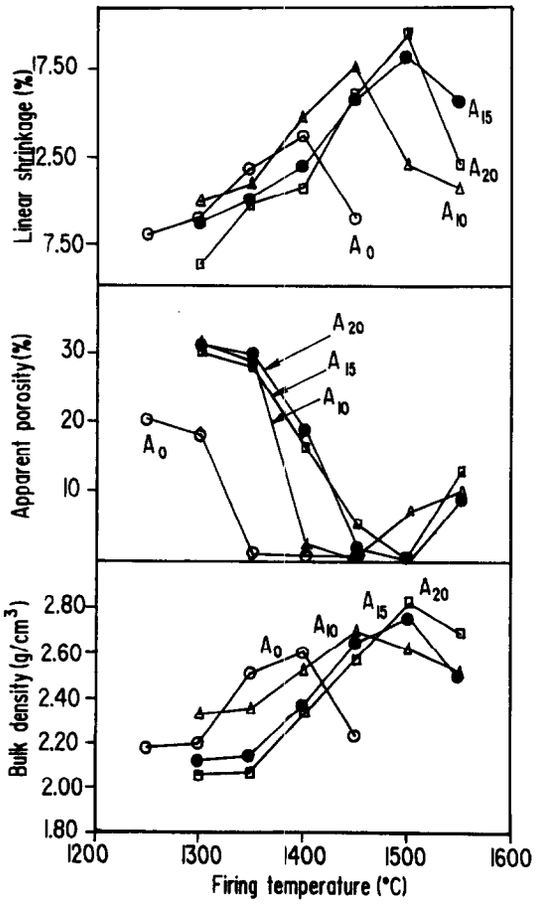


**Fig. 1.** Vitrification behaviour of porcelain compositions.

### 3.2 Densification and flexural strength

To discuss the degree of densification relative density rather than bulk density must be compared, because the contents of the crystalline phases differed in their compositions. Figure 2 shows the relative densities of the four batches. The relative

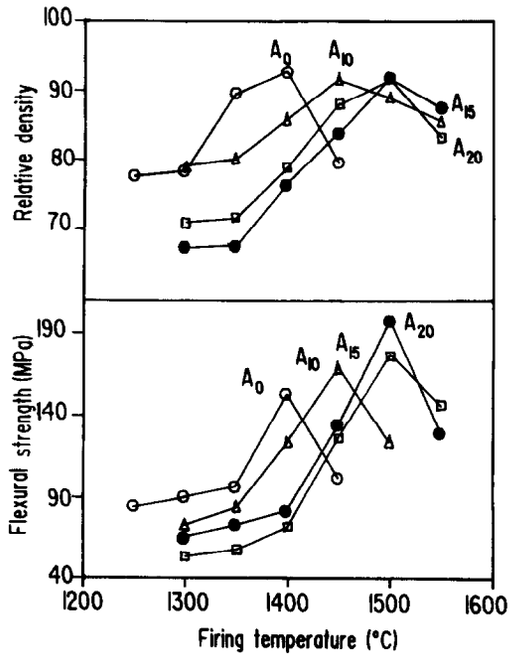


**Fig. 2.** Densification behaviour and flexural strength variation with firing temperature.

density did not vary between them; all the bodies achieved a relative density between 91 and 92%. Generally, after the apparent porosity reaches zero, the closed porosity on extended heating tends to increase because of so-called 'bloating' with an abrupt decrease in relative density. Although the closed porosity could not be measured, uniform relative density values ensured almost similar presence of closed porosity in the vitrified compositions.

In Fig. 2 the variation in flexural strength of the four compositions with increase in firing temperature is also shown. Flexural strength increased with increasing firing temperature reaching an optimum value at the respective relative density. Further heating decreased the flexural strength, similarly affecting the relative density. The temperature dependences of sintering and flexural strength were almost identical. Increased temperature of vitrification with higher alumina content was due to reduced glassy phase and increased presence of high refractory particles of alumina.

### 3.3 Effect of body composition and fired phase assemblages on mechanical properties

#### *3.3.1 Flexural strength*

Raw material compositions consisted of equal amounts of china clay and sillimanite sand, with a variation in the alumina and cordierite glass-ceramic contents. Fired compositions consisted almost wholly of mullite, undissolved sillimanite and an amorphous silica-rich phase.

With increasing alumina content replacing the cordierite glass-ceramic, the flexural strength of vitrified samples increased in a parabolic manner (Fig. 3). Increased strength was attributed to:

(i) the absence of quartz;
(ii) the formation of mullite; and
(iii) the presence of insoluble second phase.

The increase in strength with progressive substitution of cordierite glass-ceramic by alumina (Fig. 3) opposes the quartz prestressing theory.[1-4] To prove the present conclusions, alumina in $A_{15}$ was substituted completely by quartz. The drastic fall in strength confirmed that quartz does have a deleterious effect on strength when present in a porcelain composition.

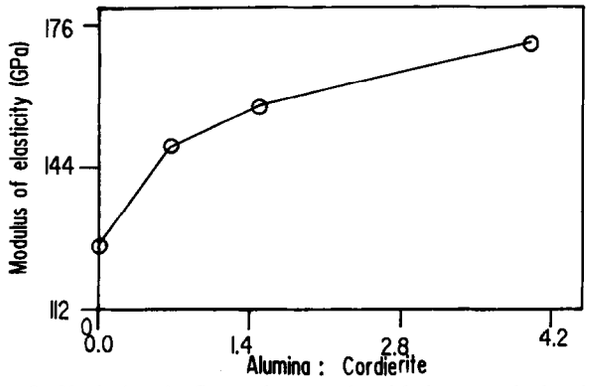


Fig. 3. Variation in flexural strength with increased alumina content.

Mullite in these compositions was formed from decomposition of the clay. With increased vitrification temperature, fine acicular needles of mullite dissolved and recrystallized as a stouter form. Thus the reported increase in strength was partly due to the stouter morphology of mullite needles. However, the observed variation in strength was also governed to a great extent by other factors, as the highest strength samples ($A_{20}$) showed no trace of mullite needles even when examined microscopically.

Increased strength in the present compositions was mainly due to a dispersion-strengthened glassy matrix reinforced by high-strength alumina and sillimanite particles dispersed within the glass. These particles acted as a barrier to crack propagation when a stress was applied and also limited the size of Griffith's flaws, thereby increasing strength.

An additional factor for increased strength was the incorporation of cordierite glass-ceramic in place of feldspar which, due to controlled crystallization during cooling, led to the formation of high-strength microcrystalline structures.

#### *3.3.2 Modulus of elasticity (MOE)*

Figure 4 shows the effect of increasing alumina content (in lieu of cordierite glass-ceramic) on the MOE of vitrified specimens. With increasing alumina content MOE increased in a parabolic manner. Since elasticity depends on the amount and nature of porosity, its dependence on porosity is also shown in Fig. 5. This plot showed an inverse linear dependence between elasticity and porosity, as expected. The widely held view that Young's modulus is directly proportional to the flexural strength[12] has also been confirmed here. Factors responsible for increased strength also governed the increase in MOE values.

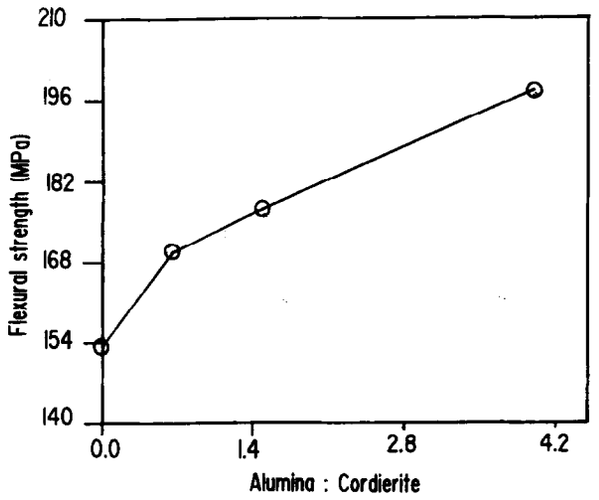


Fig. 4. Variation in MOE with increasing alumina content.

*3.3.3 Microhardness and fracture toughness*

Recently large toughness improvements were reported during the design of new microstructures consisting of refractory particles dispersed as a second phase in a ceramic matrix. According to Rice,[19] significant toughness improvements require (1) that the diameter of the particles should be smaller than the typical flaw size in the ceramic matrix (≅ 20–50 $\mu$m) and (2) that the second phase should be dense and uniform in order to reduce the interparticle distance to a dimension smaller than the typical flaw size of the matrix.[20]

With increased replacement of cordierite glass-ceramic by alumina, both the microhardness and fracture toughness increased considerably (Fig. 6) compared with those of conventional triaxial whiteware composition. Increase in microhardness values on gradual substitution of cordierite glass-ceramic by alumina was due to the presence of high-hardness and high-modulus sillimanite and alumina dispersoids embedded in a highly viscous glassy matrix.

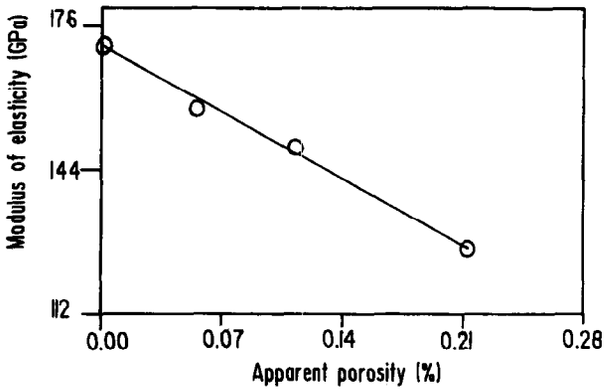


**Fig. 5.** Dependence of MOE on apparent porosity in vitrified samples.

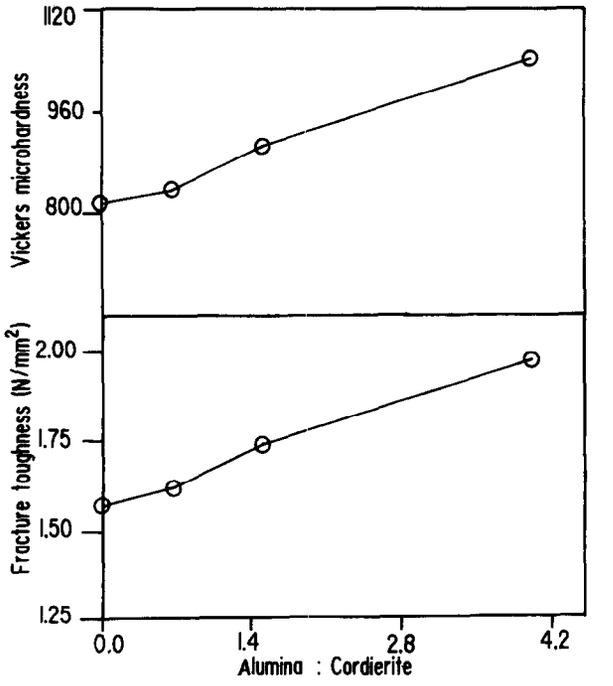


**Fig. 6.** Variation of Vicker's microhardness and fracture toughness with increasing replacement of cordierite glass-ceramic by alumina.

Increased toughness of vitrified specimens with increased alumina additions was due to crack impediment and deflection phenomena in a dispersion-strengthened high-viscous glassy matrix. This mechanism requires a fracture-resistant second phase, such as refractory particles (sillimanite and alumina particles in the present compositions) and is highly dependent on the dispersoid–matrix property mismatch.[21] The initial crack could be deflected by sufficiently weakened dispersoid–matrix interfaces which were preferred crack paths. The model of Faber and Evans[20] indicated that there was about a 100% increase in the toughness values for particulate composites reinforced with spherical particles like alumina, sillimanite or small rods of mullite with an aspect ratio lower than about 3. Disc-shaped particles also have a considerable effect on composite toughening.

## 4 Conclusion

Replacement of quartz and feldspar by sillimanite sand and alumina/cordierite glass-ceramic, respectively, in a conventional porcelain composition increased both the physical and mechanical properties of the fired bodies. Increased shrinkage values at higher alumina additions (replacing cordierite glass-ceramic) denoted a greater densification and lesser formation of porosity. At lower temperatures of firing, mullite formation aids in increasing strength. At higher firing temperatures (1500°C), although mullite dissolved in the glass, increased strength was due to a dispersion-strengthened glassy matrix. Rounded particles of sillimanite and alumina acted as dispersoids and helped in inhibiting crack propagation, thus increasing both the strength and fracture toughness values. Lowering of Griffith's flaws was also favourable in improving the mechanical properties.

## Acknowledgements

The authors are deeply indebted to Shri. S. Mondal for sample extrusion and pressing, and Shri. D.K. Naskar for machining of green samples. Thanks are also due to the Council of Scientific & Industrial Research, Govt of India, for providing financial assistance in the form of a research fellowship grant during the course of the work.

## References

1. Mattyasovsky-Zolsnay, L., Mechanical strength of porcelain. *J. Am. Ceram. Soc.*, **40** (1957) 299–306.

2. Winterling, A., Structure stress as the cause of increasing strength in porcelain. *Ber. Deut. Keram. Ges.*, **38** (1961) 9–22.
3. Dietzel, A., Significance of equilibrium diagrams for ceramics. *Sprechsaal*, **86** (1953) 251–252.
4. Marzhal, H., Influence of quartz on the strength of porcelain. *Ber. Deut. Keram. Ges.*, **32** (1955) 203–211.
5. Weidmann, T., Strength carriers in porcelain. *Sprechsaal*, **92** (1959) 2–5; 29–30; 52–55.
6. Weyl, D., Influence of internal strains on the texture and mechanical strength of porcelains. *Ber. Deut. Keram. Ges.*, **36** (1959) 319–324.
7. Warshaw, S. I. & Seider, R., Comparison of strength of triaxial porcelain containing alumina and silica. *J. Am. Ceram. Soc.*, **50** (1967) 337–343.
8. Schroeder, J. E., Inexpensive high strength electrical porcelain. *Am. Ceram. Soc. Bull.*, **57** (1978) 526.
9. Palatzky, A. & Werner, T., Increasing the mechanical strength of porcelain bodies. *Silikat. Tech.*, **9** (1958) 68–73.
10. Khandelwal, S. K. & Cook, R. L., Effect of alumina additions on crystalline constituents and fired properties of electrical porcelains. *Am. Ceram. Soc. Bull.*, **49** (1970) 522–526.
11. Kobayashi, Y., Ohira, O., Satoh, T. & Kato, E., Compositions for strengthening porcelain bodies in alumina–feldspar–kaolin system. *Trans. Brit. Ceram. Soc.*, **93** (1994) 49–52.
12. Frith, V., Heckroodt, R. O. & Schuller, K. H., The mechanical properties of zircon–feldspar porcelains. *Cfi/Ber. DKG.*, **64** (1987) 379–383.
13. Blodgett, W. E., High strength alumina porcelains. *Am. Ceram. Soc. Bull.*, **40** (1961) 74–77.
14. Maiti, K. N. & Kumar, S., Microstructure and properties of a new porcelain composition containing crystallizing glasses as replacement for feldspar. *Trans. Brit. Ceram. Soc.*, **91** (1992) 19–24.
15. Maiti, K. N. & Kumar, S., Effect of substitution of quartz by beach sand sillimanite on the properties of conventional porcelain. *Trans. Bri. Ceram. Soc.*, **89** (1990) 24–27.
16. Avgustinik, A. I. & Sintsova, I. T., Increasing the mechanical strength of porcelain by substituting crystallizing glass for quartz. *Glass & Ceramics*, **24** (1967) 322–326.
17. Hasselman, D. P. H. & Fulrath, R. M., Proposed fracture theory of dispersion-strengthened glass matrix. *J. Am. Ceram. Soc.*, **49** (1966) 68–72.
18. Evans, A. G. & Wilshaw, T. R., Quasi-static solid particle damage in brittle materials. *Acta. Metall.*, **24** (1976) 939–940.
19. Rice, R. W., Mechanisms of toughening in ceramic matrix composites. *Ceram. Eng. Sci. Proc.*, **6** (1985) 589.
20. Faber, K. T. & Evans, A. G., Crack deflection processes. *Acta Metall.*, **31** (1983) 565.
21. Lange, F. F., The interaction of a crack front with a second phase dispersion. *Phil. Mag.*, **22** (1970) 983.